

DETECTING ACTIVE ASTEROIDS/COMETS FROM OSSOS SURVEY IMAGES

AUTHORS

Affiliations

Draft version April 9, 2015

ABSTRACT

Abstract.

Keywords: keywords

1. INTRODUCTION

The active asteroids are small bodies in the main asteroid belt which have transient dust emission producing comet-like comae and tails. Unlike comets, which originate in the Kuiper Belt and Oort cloud, and have been scattered inwards by gravitational effects, the active asteroids have stable orbits confined to the main belt and likely formed in the same location as they reside presently (Scott Sheppard 2014) (?). For objects which formed in the the outer region of the main belt, beyond the snow line, the crystallized water ice which was present at the time of formation and not exposed to primordial heating may still remain in reservoirs beneath the surface (S. Sonnett 2011). According to models done by Fraser Fanale (1989), beyond heliocentric distances of 2.4 AU ice can be protected against sublimation by a 'relatively thin' surface regolith of depth 1 – 100 m for the entire age of the solar system. If the ice layer were to be exposed to sub solar heating, sublimation could be triggered, ejecting dust particles from the surface producing a coma. The source of the dust emission may be different for each object and could include ice sublimation, impact ejecta, rotational instabilities due to YORP torques, or a combination of several effects. (Henry Hsieh 2015). As the source of the observed activity may not be a result of cometary ice sublimation, these objects are better known as active asteroids. Main belt comets are a subset of this group where ice sublimation is thought to be the source of the dust emission.

Since the first discovery of an active main-belt asteroid, 133P/Elst-Pizarro, several attempts have been made to identify new objects of this type; at present, eighteen objects have been identified (refer to Figure 1) (David Jewitt 2015). A comprehensive review of such searches can be found in Henry Hsieh (2015). A persistent challenge to this effort is that the detection of the coma or tails around small dark objects is highly dependent on the magnitude constraints of the survey. As most asteroids fall near the limiting magnitude of the survey in which they are discovered (David Jewitt 2015), objects which are larger, closer, or have higher albedo are preferentially detected and any dust emission would be more easily apparent. The active fraction of identified active asteroids greater than 1 km to main belt asteroids greater than 1 km is $f \sim 10^5$, and describes a strong lower limit as many objects are yet undetected. (David Jewitt 2015)

In this paper, we present a study using the Canada-France-Hawaii Telescope (CFHT) Outer Solar System Origins Survey (OSSOS) data to identify the presence of

cometary activity in previously discovered asteroids. We select the Hungaria family as the test group for our search pipeline. Previously undetectable emission activity may be able to be identified from this data set, which was designed to detect trans neptunian objects, as the limiting magnitude (24.5 mag) is much lower than previous surveys. The survey covers a wide field of both the ecliptic plane and low inclinations, and observes with long (> 287 s) exposures, allowing for the potential serendipitous discovery of active dust emission which was previously too faint to detect. In this study we intend to observe a number of asteroids in the OSSOS data set and identify potential activity by measuring the asteroidal point spread function (PSF) and comparing this to a computed stellar model PSF in order to detect a large deviation potentially characteristic of a coma or jet around the asteroid. Objects which indicate activity are then visually examined.

2. OBSERVATIONS

Observations taken by OSSOS with the CFHT MegaPrime wide-field optical imaging facility at the summit of Mauna Kea, Hawaii, have been collected since 2013. The wide-field imager, MegaCam, consists of a 36 CCD image plane, each 2048 x 4125 CCD with resolution of 0.185"/pix. This covers a field of roughly $1^\circ \times 1^\circ$ on the sky. Each block of data taken consists of a mosaic of 21 segments of one-square-degree sky coverage, and at present, covers two orbital phase spaces on the plane of the ecliptic, and two off plane at low inclinations. MegaCam observes in the optical to near infrared with filters u^* , g' , r' , i' , and z' . Of these, r' and u^* are the best suited filters for observing main belt objects, and the analysis presented only includes observations made using these filters. [todo: reword]

The OSSOS images are reduced ... [todo: how reduced]. (standard data detrending???) Source characteristic measurements were obtained from source extraction (?) and were used to extract the orbital information the transient object.

3. ANALYSIS

From the calculated arcs provided by SSOIS (?) of objects identified as asteroids in the AstDys catalogue (?) we were able to predict which asteroids were present in the OSSOS data set, and select these objects to be examined for cometary activity. From a set of 3528 images with exposure times greater than 200s, there are [todo: fill in] observations of [todo: fill in] asteroids in the OSSOS data. We analyze a small group of objects in

the Hungaria family as our test case for our automated pipeline. Of the 1187 Hungarias we have 76 observations of 25 objects.

3.1. Object identification

An automated pipeline was written to identify each asteroid in an OSSOS exposure by, in order of 'priority': it's location relative to the predicted coordinates, elongation due to trailing effects due to the long exposure times, and apparent magnitude. The location of each object in the exposure was obtained from photometric software (?) and objects which were closest to the predicted location were chosen as asteroid candidates. The elongation condition was calculated from the predicted motion of the asteroid over the length of the exposure (?), and approximated as an ellipse which could be compared to the shape parameters calculated by the photometry. The objects were also subject to a magnitude constraint, albeit with an acknowledged large uncertainty for two reasons. The first is because objects which are active and have jets or a coma will appear brighter than the expected magnitude calculated from previous observations. Depending on the extent of the activity, this could cause the object to be measured as several magnitudes greater than predicted. And second, objects which are moving faster during the exposure, and thus trailed to a greater extent, will have their flux spread over a larger more oblong area. As the photometry software magnitude measurements are optimized for point like sources and extended objects such as galaxies, we expect a correlation between elongation and the probability of flux measurement error. For these reasons an uncertainty of 2 magnitudes was arbitrarily chosen, and as the information is not necessarily indicative of an accurate identification, an object which did not meet this condition was not rejected nor flagged. Alternatively, asteroids which were not the expected shape, but satisfied the coordinate and magnitude condition were flagged for human inspection. Cases of the asteroid being too close to bad pixels, the edge of the CCD, or involved with bright sources would be removed at this step of the pipeline. For exposures where the elongation ratio was greater than 1:5 [todo: check value, implement] the photometry measured the asteroid as two separate sources, and the image was flagged for human inspection. If more than one source met the same level of criteria but the object was not expected to be greatly elongated, the image was flagged separately for review.

In order to accurately measure the PSF of the asteroid, which is necessary to check for anomalous flux surrounding the object that could indicate activity, it is necessary to ensure that the asteroid is isolated from other sources. This was preformed with a comparison with a catalogue of bright sources built for the OSSOS images (?) in the region surrounding the asteroid, and the cases where the asteroid was involved were discarded.

To ensure that every asteroid could be accounted for in the pipeline process, exposures where no source was found by the photometry in the region surrounding the predicted location of the asteroid, no objects met the

elongation nor magnitude conditions, and images which failed to be processed by the photometry were also recorded to be reprocessed.

Applying this identification process left [fill in] objects to be examined.

3.2. PSF comparison

A postage stamp of size 2.5 times the full-width-half-maximum (FWHM) and centered on the midpoint of the elongated shape was rotated according to the angle of trailing, and a brightness profile was measured of the background subtracted data. Due to saturation effects, asteroids with magnitudes greater than 18.5 were not analyzed for activity. However, as previous surveys have included this set of objects [fill in: what surveys?] we were comfortable with this exclusion. The PSFs were then compared to the stellar model PSFs built from the OSSOS MOP (?) which were rotated by the same angle. A 3 sigma difference between the subtracted PSFs was used to indicate the presence of additional flux around an asteroid. There were [fill in] asteroids which were measured to be above this limit and were flagged for visual confirmation.

3.3. Detection Efficiency

4. DISCUSSION

As the involvement check was preformed using a catalogue of bright objects, it is possible that some asteroids identified and carried through the pipeline process were involved with dim background objects. An example of this is shown in figure 3. Depending on the geometry of the involvement this could be selected as an asteroid with activity, possibly a large bright jet. In order to distinguish between activity and involvement, the asteroids with unusual PSF's were all manually reviewed. Through this process we could determine whether a jet was present, in which case the outflowing dust would also have a trailing effect through the exposure, or if it were a case of involvement. We do not expect that a jet would be present for a fraction of the exposure time during one observation.

Acknowledgments.

REFERENCES

- The iau minor planet center.
<http://www.minorplanetcenter.net/iau/MPCORB.html>.
Accessed: 2015-01-15.
- Jessica Agarwal David Jewitt, Henry Hsieh. The active asteroids. *arXiv:1502.02361v1 [astro-ph.EP]*, 2015.
- James Salvail Fraser Fanale. The water regime of asteroid (1) ceres. *Icarus*, 1989.
- R.J. Wainscoat Henry Hsieh, L. Denneau. The main-belt comets: the pan-starrs1 perspective. *Icarus*, 2015.
- R. Jedicke S. Sonnett, J. Kleyna. Limits on the size and orbit distribution of main belt comets. *arXiv:1108.3095v1 [astro-ph.EP]*, 2011.
- Chadwick Trujillo Scott Sheppard. Discovery and characteristics of the rapidly rotating active asteroid (62412) 2000 sy178 in the main belt. *arXiv:1410.1528 [astro-ph.EP]*, 2014.

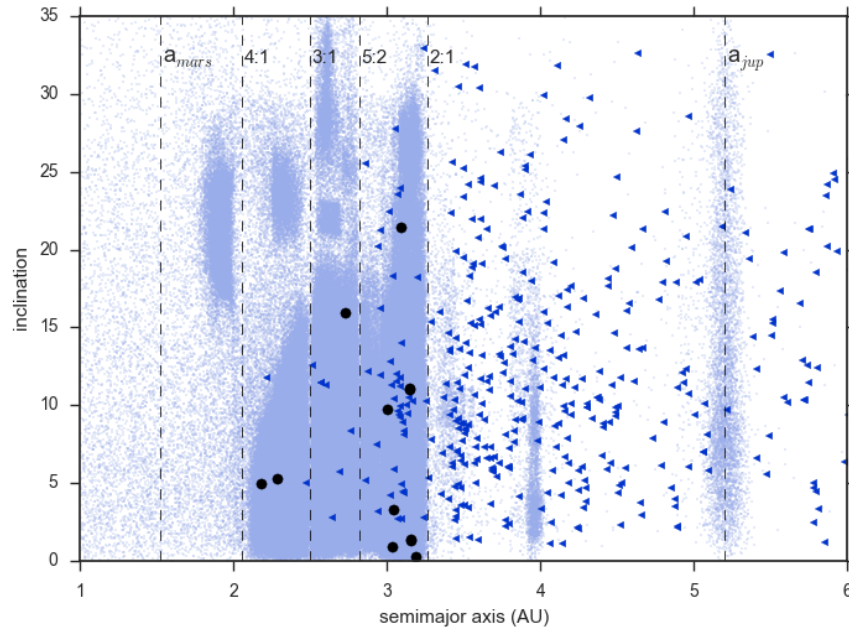


Figure 1. Inclination of all known objects in the main asteroid belt as a function of semimajor axis. Mean motion resonances between Mars and Jupiter as well as the planet's semimajor axis are marked in dashed lines, main belt objects are marked as light small dots, comets as arrows, and active asteroids as stars. [mpc](#)

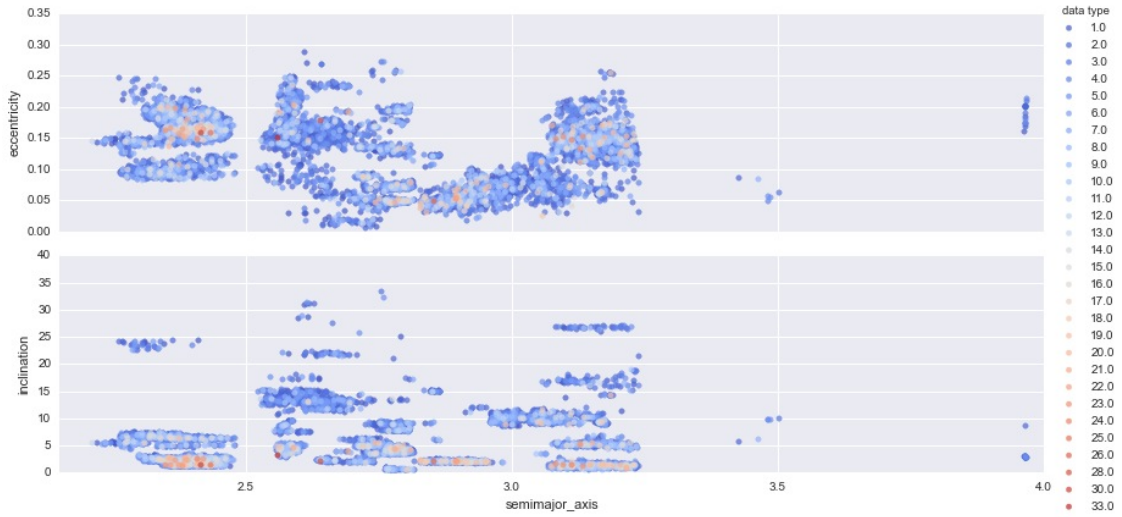


Figure 2. Inclination and eccentricity as a function of semi-major axis of all objects. Colours represents number of observations (occurrences) used in the analysis

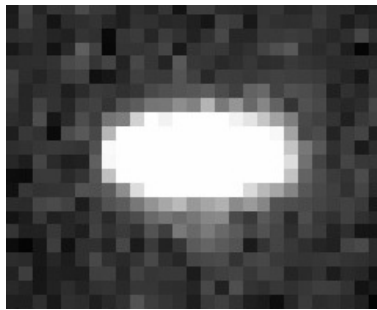


Figure 3. An asteroid involved with a dim background object.